Acta Crystallographica Section D
Biological Crystallography
ISSN 0907-4449

Structural studies of a bifunctional inhibitor of neprilysin and DPP-IV

Christian Oefner,‡ Sabine Pierau,§ Henk Schulz‡ and Glenn E. Dale*‡

Morphochem AG, CH-4058, Basel, Switzerland

‡ Present address: Arpida AG, Reinach, Switzerland.
§ Present address: Huntsmann, Basel, Switzerland.

Correspondence e-mail: glenn.dale@arpida.com

Received 12 June 2007
Accepted 24 July 2007

PDB Reference: neprilysin–MCB3937 complex, 2qpj, r2qpjsf.

Neutral endopeptidase (NEP) is the major enzyme involved in the metabolic inactivation of a number of bioactive peptides including the enkephalins, substance P, endothelin, bradykinin and atrial natriuretic factor, as well as the incretin hormone glucagon-like peptide 1 (GLP-1), which is a potent stimulator of insulin secretion. The activity of GLP-1 is also rapidly abolished by the serine protease dipeptidyl peptidase IV (DPP-IV), which led to an elevated interest in inhibitors of this enzyme for the treatment of type II diabetes. A dual NEP/DPP-IV inhibitor concept is proposed, offering an alternative strategy for the treatment of type 2 diabetes. Here, the synthesis and crystal structures of the soluble extracellular domain of human NEP (residues 52–749) complexed with the NEP, competitive and potent dual NEP/DPP-IV inhibitor MCB3937 are described.

1. Introduction

A significant and rapidly growing fraction of the human population is affected by type 2 diabetes, a disease characterized by elevated blood glucose levels and relative insulin insufficiency. Glucose-dependent insulin secretion is promoted by incretin hormones, predominantly glucose-dependent insulinotropic peptide (GIP) and glucagon-like peptide 1 (GLP-1). The available evidence suggests that enhancement of incretin action may be useful for lowering blood glucose in subjects with type 2 diabetes mellitus (Drucker, 2003).

The activity of the potent stimulators of insulin secretion, GLP-1 and GIP, is rapidly abolished by truncation mediated by the serine protease dipeptidyl peptidase IV (DPP-IV, CD26; EC 3.4.14.5). DPP-IV has multiple properties and modulates the biological activity of several peptide hormones, chemokines and neuropeptides by specifically cleaving after a proline or alanine at amino-acid position 2 from the N-terminus (Mentlein, 1999). *In vivo* administration of synthetic inhibitors of DPP-IV prevents N-terminal degradation of GLP-1 and GIP, resulting in higher plasma concentrations of these hormones, increased insulin secretion and therefore improved glucose tolerance (Marguet *et al.*, 2000). This has led to an elevated interest in inhibitors of this enzyme for the treatment of type II diabetes. GLP-1 levels fall rapidly following postprandial excursion and clearance reflects the actions of the kidney: enzymatic inactivation by DPP-IV as well as neutral endopeptidase (NEP) 24.11 (Plamboeck *et al.*, 2003; Hupe-Sodmann *et al.*, 1995, 1997), where NEP is responsible for fast renal elimination of GLP-1 with 50–70% extraction. An improvement in GLP-1 stability has been

demonstrated by a combined inhibition of NEP and DPP-IV in anaesthetized pigs (Plamboeck *et al.*, 2003). Plamboeck and coworkers have shown that treatment of diabetic rats with a combination of a DPP-IV inhibitor and an NEP inhibitor results in glucose-lowering effects that are superior to those observed using only a DPP-IV inhibitor. It is proposed that mixed inhibition of NEP and DPP-IV offers an alternative strategy for the treatment of type 2 diabetes.

DPP-IV (CD26; EC 3.4.14.5) is a multifunctional type II transmembrane serine protease glycoprotein 766 amino acids in length, with six amino acids in the cytoplasm, 22 residues spanning the plasma membrane and 738 amino acids comprising the extracellular domain (Misumi *et al.*, 1992). DPP-IV has multiple properties including highly specific serine protease activity that cleaves N-terminal dipeptides from peptides with an L-proline or L-alanine as the penultimate residue, inactivating or generating biologically active peptides (Torimoto *et al.*, 1992; Mentlein, 1999). In addition to the advances in understanding the biological functions of DPP-IV, the structural basis of the dipeptidyl peptidase activity of the enzyme and how it selectively chooses short peptides such as GLP-1 and GIP as substrates has been elucidated from three-dimensional crystal structures of the enzyme from various sources (Rasmussen *et al.*, 2003; Engel *et al.*, 2003; Oefner *et al.*, 2003; Thoma *et al.*, 2003; Aertgeerts *et al.*, 2004; Peters *et al.*, 2004; Bjelke *et al.*, 2004; Hiramatsu *et al.*, 2004).

Several classes of DPP-IV inhibitors have been described, including diprotin A and B, α-amino boronic acid analogues of proline, dipeptides, amino-acid pyrrolidides and thiazolidides, aminomethylpyrimidines, diaryl phosphonates and 2-cyano-pyrrolidines and the more recently described pyrrolidine-carbonitrile derivatives (Villhauer *et al.*, 2002; Hughes *et al.*, 1999; Stöckel-Maschek *et al.*, 2000; Flentke *et al.*, 1991). The 2-cyano-pyrrolidine derivatives were predicted to form a covalent adduct with the active-site serine of DPP-IV, forming an imidate adduct (Hughes *et al.*, 1999). This has recently been demonstrated crystallographically by Oefner *et al.* (2003).

Recently, the structure of Val-pyrrolidide-inhibited DPP-IV has been reported, providing insight into the fold of the enzyme and indicating how substrate specificity is achieved (Rasmussen *et al.*, 2003). The pyrrolidide moiety is buried in a narrow hydrophobic pocket next to the active serine, restricting the possible residues at the P_1 position in substrates. The valine side chain of the P_2 residue points towards a large cavity and does not make specific contacts with DPP-IV. The extended size of the unprimed subsite region in DPP-IV has been demonstrated upon binding of the iodinated variant of the inhibitor NVP-DPP728 (Oefner *et al.*, 2003).

Neprilysin (NEP; EC 3.4.24.11), also known as neutral endopeptidase, enkephalinase, CALLA or CD10, is the prototype of the M13 subfamily of type II integral membrane zinc-dependent endopeptidases. It was originally extracted and purified from the brush border of rabbit kidney and is a peptidase capable of hydrolyzing insulin B chain (Kerr & Kenny, 1974). The catalytic properties of NEP resemble those of a group of zinc-dependent bacterial endopeptidases, of which thermolysin (TLN) is the best characterized (Holmes & Matthews, 1982). NEP is located at the cell surface, with the bulk of the protein, including the active site, facing the extracellular space, and therefore functions as an ectoenzyme catalyzing peptide hydrolysis at the surface of the plasma membrane. It is widely distributed in mammalian tissues and is involved in the inactivation of a variety of signalling peptides (Erdos & Skidgel, 1989; Roques *et al.*, 1993; Turner & Tanzawa, 1997). NEP has been implicated in the regulation of opioid peptide action through the degradation of endogenously released enkephalins (Roques *et al.*, 1980). NEP is involved in the physiological degradation of the peptides modulating blood pressure, such as the cardiac hormone atrial natriuretic peptide (ANP), bradykinin and endothelin. More recently, NEP has been implicated in the degradation of amyloid β peptide (Aβ1–42), the primary pathogenic agent in Alzheimer's disease (Shirotani *et al.*, 2001; Iwata *et al.*, 2001), and has been shown to play a role in the degradation of the incretin hormone glucagon-like peptide 1 (GLP-1), which is a potent stimulator of insulin secretion. To date, potent inhibitors of NEP have been synthesized that produce a pharmacological response through an increase in opioid or vasoactive peptide levels, indicating their therapeutic potential as novel analgesics or antihypertensive agents (Burnett, 1999; Roques & Beaumont, 1990).

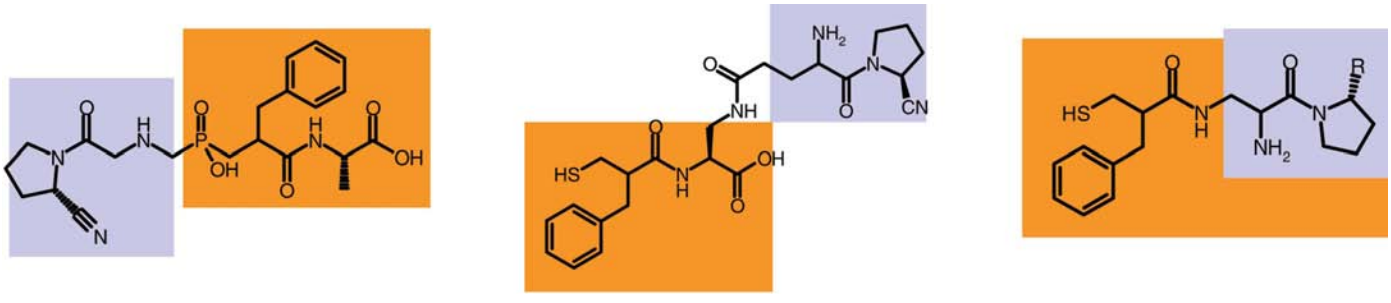

Figure 1
Potential bifunctional molecules. The NEP-inhibitor component is highlighted in orange and the cyano-pyrrolidide component of the DPP-IV inhibitor is highlighted in cyan.

The recent elucidation of the structure of the soluble extracellular domain (Asp52–Trp749) of human NEP (sNEP) determined in complexes with phosphoramidon (Oefner *et al.*, 2000) and with specific and potent inhibitors (Oefner *et al.*, 2004) as well as with a nonpeptidic neprilysin inhibitor (Sahli *et al.*, 2004) has provided insight into the subsite specificity of this enzyme and has supported much of the earlier biochemical and modelling data (Tiraboschi *et al.*, 1999). Extensive studies of enkephalin analogues and dipeptides have shown that the specificity of NEP is essentially ensured by the S_1' subsite, which interacts primarily with aromatic or large hydrophobic residues. However, the binding of the first potent synthetic NEP inhibitor, thiorphan {*N*-[(*R*,*S*)-(3-mercapto-2-benzyl-propanoyl)]-glycine} (K_i = 4 n*M*), demonstrates the energetically greater importance of the zinc-coordinating thiol group compared with the stereochemically dependent van der Waals interactions in subsite recognition for small-molecule binding (Fournie-Zaluski *et al.*, 1985; Gaucher *et al.*, 1999; Dale & Oefner, 2004). The S_2' subsite of NEP shows reduced specificity and can accommodate bulkier side chains. Smaller P_1' substituents allow the presence of both smaller or larger P_2' residues (Oefner *et al.*, 2004). In contrast to the stringent S_1' specificity of NEP, there is only a minor stabilizing role of the S_1 subsite upon inhibitor binding.

Based on structural knowledge of human NEP and human DPP-IV, in particular the understanding of their subsite specificity, a dual inhibition concept similar to that described by Fournie-Zaluski can be envisioned (Roques, 1993; Chen *et al.*, 2000). Inhibitors of DPP-IV can be linked *via* their terminal unprimed substituent with NEP inhibitors *via* their terminal unprimed residue, their two-primed residue or the C-terminal moiety. This dual-inhibition concept leads to chemical arrangements of the NEP inhibitor thiorphan and the cyano-pyrrolidide inhibitor of DPP-IV as exemplified in Fig. 1.

In order to identify the intermolecular interactions of a bifunctional NEP/DPP-IV inhibitor with the respective enzymes and to further understand the mode of enzyme inhibition with the aim of designing novel NEP/DPP-IV inhibitors that are active *in vivo*, a bifunctional inhibitor has been synthesized (Fig. 2) and a binary complex with NEP has been solved by X-ray crystallography using the protein coordinates of sNEP present in a complex with phosphoramidon (PDB code 1dmt) as the starting model. The soluble extracellular domain of human NEP was expressed in yeast and the protein was purified to homogeneity as described in Dale *et al.* (2000). Crystals could be obtained for the Endo F1 glycosidase-treated enzyme in the presence of the inhibitor.

Table 1
Data-collection and refinement statistics.

Values in parentheses are for the outer resolution shell.

Wavelength (Å)	1.54
Temperature (K)	100
Space group	$P3_221$
Unit-cell parameters (Å)	a = 107.12, b = 113.37
Resolution range (Å)	20.0–2.05 (2.12–2.05)
No. of observed reflections	116329
No. of unique reflections	43955
R_{sym}† (%)	6.2 (51.5)
$I/\sigma(I)$	10.7 (1.8)
Completeness (%)	93.2 (85.6)
Refinement statistics	
Resolution range (Å)	20–2.05
R_{cryst}/R_{free}‡ (%)	20.7/26.8
No. of protein atoms	5595
Mean B (Å^2)	28.2
No. of water molecules	295
No. of ligand atoms	29
Mean B (Å^2)	20.0
No. of NAG atoms	42
Mean B (Å^2)	43.7
R.m.s.d.§ bonds (Å^2)	0.005
R.m.s.d.§ angles (°)	0.737

† $R_{sym} = \sum_h \sum_i |I_i(h) - \langle I(h)\rangle| / \sum_h \sum_i I_i(h)$, where $I_i(h)$ and $\langle I(h)\rangle$ are the ith and mean measurement of the intensity of reflection h. ‡ $R_{cryst} = \sum_h ||F_{obs}| - |F_{calc}|| / \sum_h |F_{obs}|$, where $|F_{obs}|$ and $|F_{calc}|$ are the observed and calculated structure-factor amplitudes for reflection h. R_{free} is the same but based on 5% of the data excluded from refinement. § R.m.s.d., root-mean-square deviation from mean.

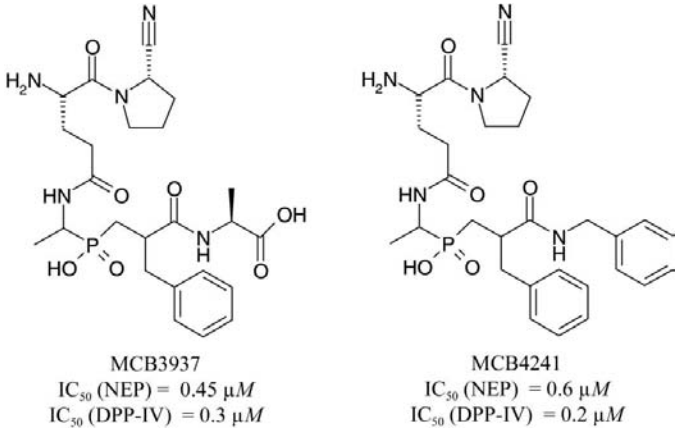

Figure 2
Chemical structure of the bifunctional NEP/DPP-IV inhibitors MCB3937 and MCB4241. The IC_{50} values for each inhibitor are indicated.

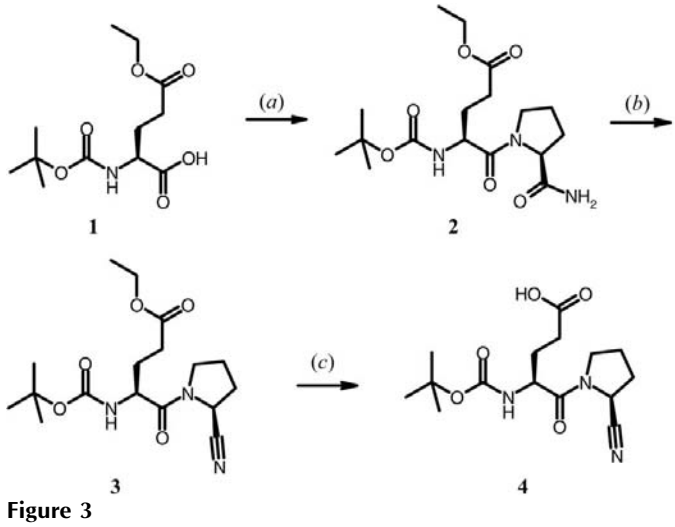

Figure 3
Synthesis of DPP-IV-inhibitory fragment **4**. Reagents and conditions: (*a*) EDCI, HOBT, L-prolinamide, *N*-methylmorpholine, DCM, room temperature, 67%; (*b*) $POCl_3$, imidazole, pyridine, 92%; (*c*) THF, 0.1 *N* LiOH, quantitative.

2. Materials and methods

2.1. Chemical synthesis of MCB3937

Following the design strategy of a bifunctional NEP/DPP-IV inhibitor, we synthesized the inhibitory fragments for both enzymes as shown in Figs. 3 and 4.

Fig. 3 shows the synthesis of the DPP-IV-inhibitory fragment **4** starting from the protected glutaric acid **1**, which was coupled with L-prolinamide under standard conditions to give compound **2**. Compound **2** was converted to the nitrile **3** using $POCl_3$ and imidazole. Subsequently, the ester side chain was saponified to give compound **4**. The synthesis of the NEP-inhibitory fragment **10** is shown in Fig. 4. The Boc-protected phosphinic acid **5** was coupled with benzacrylic acid **6** to give compound **7**, which was saponified to give compound **8**. Compound **8** was coupled with alanine methyl ester under standard conditions to give compound **9**, which after removal of the Boc protecting group gave the desired fragment **10**. The preparation of MCB3937 is shown in Fig. 5. Fragment **4** and fragment **10** were coupled under standard conditions to give compound **11**. After hydrolysis of the ester (compound **11**), the Boc protecting group was removed to give the desired final compound MCB3937.

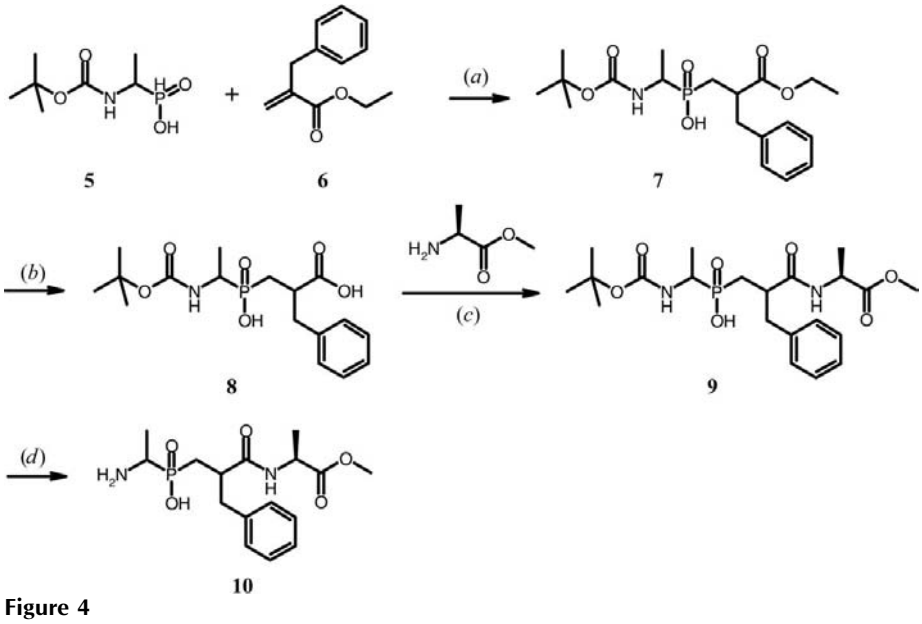

Figure 4
Synthesis of NEP-inhibitory fragment **10**. Reagents and conditions: (*a*) BSA, 5 d, 86%; (*b*) 1 *N* NaOH, ethanol, quantitative; (*c*) BOP, Et_3N, DMF, 72%; (*d*) 1.25 *M* HCl in MeOH, quantitative.

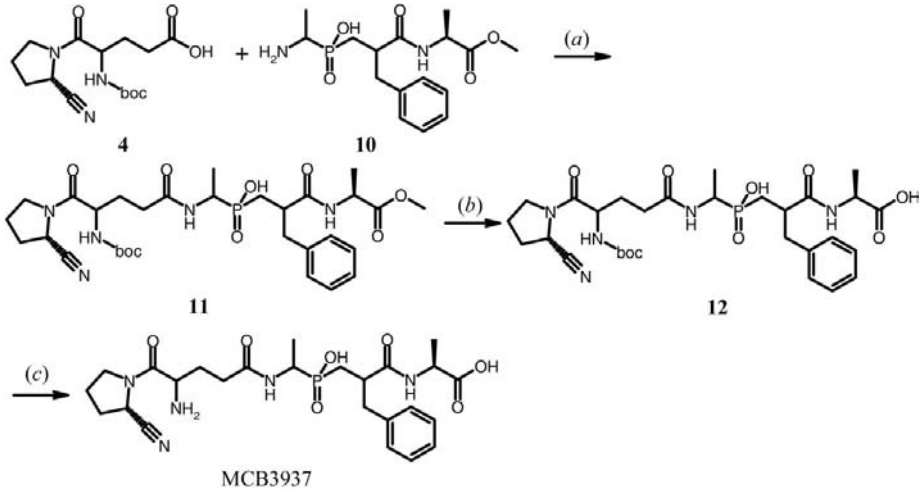

Figure 5
Preparation of MCB3937. Reagents and conditions: (*a*) EDCI, HOBT, *N*-methylmorpholine, DCM, 57%; (*b*) NaOH, EtOH, 87%; (*c*) TFA, quantitative.

2.2. Crystallization, data collection and refinement

The protein was concentrated to 20 mg ml^{-1} in 25 m*M* Tris pH 7.0, 150 m*M* NaCl and 2 m*M* $MgCl_2$ and was treated with Endo F1 glycosidase to remove N-linked sugars as described by Gruenunger-Leitch *et al.* (1996). A binary complex of the glycosidase-treated sNEP was formed with the bifunctional NEP/DPP-IV inhibitor MCB3937 at a concentration of 5 m*M*. No zinc was added to the protein solution. Crystals of the inhibited protein were obtained using the hanging-drop vapour-diffusion method with 25% PEG 3350, 200 m*M* ammonium sulfate buffered with 100 m*M* bis-Tris pH 7.5 (Dale *et al.*, 2000). The trigonal crystals, isomorphous to those obtained for the binary complex with phosphoramidon, belonged to space group $P3_221$ and contained one molecule of inhibited protein in the asymmetric unit. A crystal was flash-frozen in a cryoprotectant solution corresponding to the reservoir conditions containing 30% glycerol and data were collected at 100 K using a MAR 345 image-plate area detector mounted on a Nonius FR591 rotating-anode generator equipped with Osmic focusing mirrors. The data were processed and scaled using *DENZO* and *SCALEPACK* (Otwinowski, 1993) and analyzed further using the *CCP*4 program suite (Collaborative Computational Project, Number 4, 1994). The structure was solved by molecular replacement using the refined protein coordinates of human sNEP complexed with phosphoramidon (PDB code 1dmt; Oefner *et al.*, 2000), which was originally determined in a different crystal setting. Stereochemically restrained positional and temperature-factor refinement was performed with *REFMAC* (Murshudov *et al.*, 1997), using parameters for ideal stereochemistry as described by Engh & Huber (1991). Model building was

performed with *MOLOC* (Gerber, 1992). A difference Fourier map unequivocally revealed residual electron density located in the active site corresponding to the bound bifunctional inhibitor. Progressive introduction of solvent molecules with good geometry led to a binary complex lacking the two N-terminal residues Asp52 and Asp53. N-glycosylation on Asn144, Asn304 and Asn627 is confirmed by electron density consistent with a single *N*-acetyl-glucosamine (NAG) moiety as previously described (Oefner *et al.*, 2000). Data-collection and refinement statistics are summarized in Table 1.

3. Results and discussion

MCB3937 and MCB4281 inhibit both DPP-IV and NEP with IC_{50} values in the nanomolar range (Fig. 2). The inhibition patterns of the compounds were typical of competitive inhibitors when analyzed using Dixon and Cornish–Bowdon plots (Cortes *et al.*, 2001). MCB3937 binds to NEP near the conserved residues of the consensus sequences ^{583}HE*xx*H^{587}

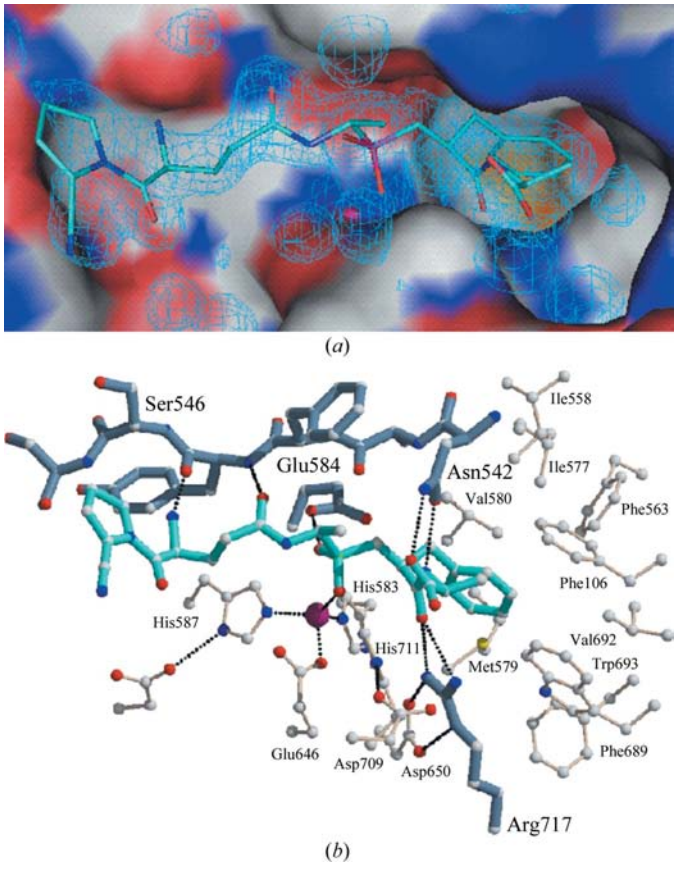

Figure 6
(*a*) $2F_o - F_c$ electron-density map for compound MCB3937 at 2.05 Å calculated using phases from the refined model. The map, contoured at 1σ, is shown as a light cyan mesh. The molecular surface is indicated and coloured by electrostatic potential: blue, positive; red, negative. The Zn atom is shown as a red sphere. The figure was generated using *PyMOL* (DeLano, 2001). (*b*) Ligand binding in the active site of human NEP. Residues directly involved in inhibitor binding *via* intermolecular hydrogen bonds are coloured dark blue. The S_1' and S_2' subsites are indicated. This figure was generated with the programs *MOLSCRIPT* (Kraulis, 1991) and *RASTER3D* (Merrit & Bacon, 1997).

and ^{646}E*xxx*D^{650} of the members of the type II integral membrane zinc-dependent endopeptidases of the M13 subfamily, which are involved in zinc binding and catalysis (Matthews, 1988). Fig. 6 shows the final electron density for the bound bifunctional inhibitor determined at 2.05 Å calculated using phases from the refined model. The inhibitor is involved in a monodentate recognition of the zinc ion involving a single oxygen (O6) of the phosphinic acid moiety. The interatomic distance to the divalent metal ion is 2.25 Å. The second oxygen of the phosphinic acid, O5, is hydrogen bonded to OE1 of the catalytic residue Glu584 at a distance of 2.57 Å and replaces the catalytic water molecule, which is polarized by the acidic amino-acid side chain during catalysis (Devault *et al.*, 1988). The coordination of the mononuclear zinc-binding site further involves the side chains of the three conserved amino-acid residues His583 (NE2), His587 (NE2) and Glu646 (OE1), with interatomic distances of 2.0, 2.13 and 1.98 Å, respectively, and is identical to that observed for phosphoramidon (Fig. 3). Furthermore, the positions of the residues involved in a complex hydrogen-bonding network around the zinc ligands remain the same within experimental error. The benzyl-propanoyl-alanine moiety of the bifunctional inhibitor, which represents the P_1' and P_2' residues, binds to NEP in a similar manner to the 2-benzyl-propanoyl-glycine moiety of thiorphan (Dale & Oefner, 2004). The benzyl moiety of the inhibitor interacts with the S_1' subsite of the enzyme, providing affinity towards NEP by interacting primarily with aromatic or large hydrophobic residues within the subsite.

The peptidic backbone of the NEP component of the inhibitor is further involved in the same intermolecular interactions as observed for phosphoramidon (Oefner *et al.*, 2000). The side chain of Arg717, which participates in a salt bridge with Asp650, interacts with the inhibitor by forming two hydrogen bonds with the carbonyl O atom of the benzyl moiety in the P_1' position. Further hydrophilic interactions are provided by the side chain of Asn542, which functions as a hydrogen-bond acceptor and donor group and interacts with the amino and C-terminal carboxyl groups of the P_2' residue of the inhibitor, with hydrogen-bonding distances of 2.71 and 2.50 Å, respectively. The carboxy-terminal L-alanine residue is recognized by residues of the S_2' subsite, which shows reduced specificity and extends into the solvent towards the side chains of Arg102, Asp107 and Arg110. Its enzyme recognition is similar to that observed previously for specific NEP inhibitors (Oefner *et al.*, 2004). In all cases the methyl moiety is within van der Waals contact distance of the side chain of Phe106. The methyl moiety of the P_1 residue, which separates the NEP from the DPP-IV inhibitory functionalities, is exposed to solvent and plays a similar role in ligand binding to that of the rhamnose moiety of phosphoramidon. It is not in direct contact with the protein, reflecting the minor stabilizing role of the S_1 subsite in NEP (Ksander *et al.*, 1997).

The cyano-pyrrolidine-glutamate dipeptide moiety represents the DPP-IV inhibitor component of the bifunctional inhibitor. It forms an amide bond with the NEP-inhibitory component *via* its glutamate side chain and is located towards the unprimed subsites in NEP by adopting an extended

conformation along β3, which contains the consensus motif ^{542}NAFY^{545} of the M13 metallopeptidase family. The free amino group of the DPP-IV-inhibitory component interacts with the carbonyl O atom of Tyr545; the side-chain O atom of the inhibitor is within hydrogen-bonding distance of NH of the same residue. The hydrogen-bonding distances are 1.99 and 2.75 Å, respectively. The cyano-pyridine moiety, which covalently interacts with the active-site serine residue 630 of DPP-IV by forming a transient imidate intermediate (Oefner *et al.*, 2003), faces towards the border of the internal active-site cavity in NEP formed by residues Asp208, Tyr346, Ser547 and Asn592. It is the most flexible fragment of the bound bifunctional inhibitor and does not enhance the binding affinity compared with thiorphan.

The crystallographic and biochemical data demonstrate that the bifunctional inhibitor MCB3957, which has been developed on the bases of structural knowledge and understanding of the subsite specificity of the target enzymes, can competitively inhibit the zinc-dependent endopeptidase NEP as well as the serine protease DPP-IV. This is to the best of our knowledge the first small molecule which inhibits two mechanistically different enzymes of the same class. The concept of dual NEP/DPP-IV inhibitors can in principle be applied to the various known inhibitor classes of the respective enzymes in order to improve the inhibitory activity.

4. Conclusions

The information provided by the three-dimensional structure of the binary complex of NEP with the bifunctional NEP/DPP-IV inhibitor MCB3937 leads to an understanding of the intermolecular interactions of the DPP-IV inhibitory component with the zinc-dependent endopeptidase. It gives insight into zinc ligation and subsite-binding motifs and presents an attractive challenge for the design of novel molecules as potential modulators for the dual NEP/DPP-IV inhibition concept for the treatment of type II diabetes.

We gratefully acknowledge Rana Gardiner for excellent technical assistance.

References

Aertgeerts, K., Ye, S., Tennant, M. G., Kraus, M. L., Rogers, J., Sang, B. C., Skene, R. J., Webb, D. R. & Prasad, G. S. (2004). *Protein Sci.* **13**, 412–421.

Bjelke, J. R., Christensen, J., Branner, S., Wagtmann, N., Olsen, C., Kanstrup, A. B. & Rasmussen, H. B. (2004). *J. Biol. Chem.* **279**, 34691–34697.

Burnett, J. C. (1999). *J. Hypertens. Suppl.* **17**, s37–s43.

Chen, H., Noble, F., Mothé, A., Meudal, H., Coric, P., Danascimento, S., Roques, B. P., George, P. & Fournié-Zaluski, M. C. (2000). *J. Med. Chem.* **43**, 1398–1408.

Collaborative Computational Project, Number 4 (1994). *Acta Cryst.* D**50**, 760–763.

Cortes, A., Cascante, M., Cardenas, M. L. & Cornish-Bowden, A. (2001). *Biochem. J.* **357**, 263–268.

Dale, G. E., D'Arcy, B., Yuvaniyama, C., Wipf, B., Oefner, C. & D'Arcy, A. (2000). *Acta Cryst.* D**56**, 894–897.

Dale, G. E. & Oefner, C. (2004). *Handbook of Metalloproteins*, Vol. 3, edited by A. Messerschmidt, W. Bode & M. Cygler, pp. 104–115. Chichester: John Wiley & Sons.

DeLano, W. L. (2001). *PyMOL.* DeLano Scientific, San Carlos, CA, USA.

Devault, A., Sales, N., Nault, C., Beaumont, A., Roques, B. P., Crine, P. & Boileau, G. (1988). *FEBS Lett.* **231**, 54–58.

Drucker, D. J. (2003). *Expert Opin. Investig. Drugs*, **12**, 87–100.

Engel, M., Hoffmann, T., Wagner, L., Wermann, M., Heiser, U., Kiefersauer, R., Huber, R., Bode, W., Demuth, H. U. & Brandstetter, H. (2003). *Proc. Natl Acad. Sci. USA*, **100**, 5063–5068.

Engh, R. A. & Huber, R. (1991). *Acta Cryst.* A**47**, 392–400.

Erdos, E. G. & Skidgel, R. A. (1989). *FASEB J.* **3**, 145–151.

Flentke, G. R., Munoz, E., Huber, B. T., Plaut, A. G., Kettner, C. A. & Bachovchin, W. W. (1991). *Proc. Natl Acad. Sci. USA*, **88**, 1556–1559.

Fournie-Zaluski, M. C., Coulaud, A., Bouboutou, R., Chaillet, P., Devin, J., Waksman, G., Costentin, J. & Roques, B. P. (1985). *J. Med. Chem.* **28**, 1158–1169.

Gaucher, J. F., Selkti, M., Tiraboschi, G., Prangé, T., Roques, B. P., Tomas, A. & Fournie-Zaluski, M. C. (1999). *Biochemistry*, **38**, 12569–12576.

Gerber, P. (1992). *Biopolymers*, **32**, 1003–1017.

Gruenunger-Leitch, F., D'Arcy, A., D'Arcy, B. & Chene, C. (1996). *Protein Sci.* **5**, 2617–2622.

Hiramatsu, H., Yamamoto, A., Kyono, K., Higashiyama, Y., Fukushima, C., Shima, H., Sugiyama, S., Inaka, K. & Shimizu, R. (2004). *Biol. Chem.* **385**, 561–564.

Holmes, M. A. & Matthews, B. W. (1982). *J. Mol. Biol.* **160**, 623–639.

Hughes, T. E., Mone, M. D., Russell, M. E., Weldon, S. C. & Villhauer, E. B. (1999). *Biochemistry*, **38**, 11597–11603.

Hupe-Sodmann, K., Goke, R., Goke, B., Thole, H. H., Zimmermann, B., Voigt, K. & McGregor, G. P. (1997). *Peptides*, **18**, 625–632.

Hupe-Sodmann, K., McGregor, G. P., Bridenbaugh, R., Goke, R., Goke, B., Thole, H., Zimmermann, B. & Voigt, K. (1995). *Regul. Pept.* **58**, 149–156.

Iwata, N., Tsubuki, S., Takaki, Y., Shirotani, K., Lu, B., Gerard, N. P., Gerard, C., Hama, E., Lee, H. J. & Saido, T. C. (2001). *Science*, **292**, 1550–1552.

Kraulis, P. J. (1991). *J. Appl. Cryst.* **24**, 946–950.

Ksander, G. M., de Jesus, R., Yuan, A., Ghai, R. D., Trapani, A., McMartin, C. & Bohacek, R. (1997). *J. Med. Chem.* **40**, 495–505.

Kerr, M. A. & Kenny, A. J. (1974). *Biochem. J.* **137**, 477–488.

Marguet, D., Baggio, L., Kobayashi, T., Bernard, A. M., Pierres, M., Nielsen, P. F., Ribel, U., Watanabe, T., Drucker, D. J. & Wagtmann, N. (2000). *Proc. Natl Acad. Sci. USA*, **97**, 6874–6879.

Matthews, B. W. (1988). *Acc. Chem. Res.* **21**, 333–340.

Mentlein, R. (1999). *Regul. Pept.* **85**, 9–24.

Merrit, E. A. & Bacon, D. J. (1997). *Methods Enzymol.* **277**, 505–524.

Misumi, Y., Hayashi, Y., Arakawa, F. & Ikehara, Y. (1992). *Biochim. Biophys. Acta*, **1131**, 333–336.

Murshudov, G. N., Vagin, A. A. & Dodson, E. J. (1997). *Acta Cryst.* D**53**, 240–255.

Oefner, C., D'Arcy, A., Hennig, M., Winkler, F. K. & Dale, G. E. (2000). *J. Mol. Biol.* **296**, 341–349.

Oefner, C., D'Arcy, A., Mac Sweeney, A., Pierau, S., Gardiner, R. & Dale, G. E. (2003). *Acta Cryst.* D**59**, 1206–1212.

Oefner, C., Roques, B. P., Fournie-Zaluski, M.-C. & Dale, G. E. (2004). *Acta Cryst.* D**60**, 392–396.

Otwinowski, Z. (1993). *Proceedings of the CCP4 Study Weekend. Data Collection and Processing*, edited by L. Sawyer, N. Isaacs & S. Bailey, pp. 56–62. Warrington: Daresbury Laboratory.

Peters, J. U., Weber, S., Kritter, S., Weiss, P., Wallier, A., Boehringer, M., Hennig, M., Kuhn, B. & Loeffler, B. M. (2004). *Bioorg. Med. Chem. Lett.* **14**, 1491–1493.

Plamboeck, A., Holst, J. J., Carr, R. D. & Deacon, C. F. (2003). *Adv. Exp. Med. Biol.* **524**, 303–312.

Rasmussen, H. B., Branner, S., Wiberg, F. C. & Wagtmann, N. (2003). *Nature Struct. Biol.* **10**, 19–25.
Roques, B. P. (1993). *Biochem. Soc. Trans.* **21**, 678–685.
Roques, B. P. & Beaumont, A. (1990). *Trends Pharmacol. Sci.* **11**, 245–249.
Roques, B. P., Fournié-Zaluski, M. C., Soroca, E., Lecomte, J. M., Malfroy, B., Llorens, C. & Schwartz, J. C. (1980). *Nature (London)*, **288**, 286–288.
Roques, R. P., Noble, F., Dauge, V., Fournie-Zaluski, M.-C. & Beaumont, A. (1993). *Pharmacol. Rev.* **45**, 87–146.
Sahli, S., Stump, B., Welti, T., Blum-Kaelin, D., Aebi, J. D., Oefner, C., Bohm, H. J. & Diederich, F. (2004). *Chembiochem*, **5**, 996–1000.
Shirotani, K., Tsubuki, S., Iwata, N., Takaki, Y., Harigaya, W., Maruyama, K., Kiryu-Seo, S., Kiyama, H., Iwata, H., Tomita, T., Iwatsubo, T. & Saido, T. C. (2001). *J. Biol. Chem.* **276**, 21895–21901.
Stöckel-Maschek, A., Mrestani-Klaus, C., Stiebitz, B., Demuth, H. & Neubert, K. (2000). *Biochim. Biophys. Acta*, **1479**, 15–31.
Thoma, R., Loffler, B., Stihle, M., Huber, W., Ruf, A. & Hennig, M. (2003). *Structure*, **11**, 947–959.
Tiraboschi, G., Jullian, N., Thery, V., Antonczak, S., Fournie-Zaluski, M.-C. & Roques, B. P. (1999). *Protein Eng.* **12**, 141–149.
Torimoto. Y., Dang, N. H., Tanaka, T., Prado, C., Schlossman, S. F. & Morimoto, C. (1992). *Mol. Immunol.* **29**, 183–192.
Turner, A. J. & Tanzawa, K. (1997). *FASEB J.* **11**, 355–364.
Villhauer, E. B., Brinkman, J. A., Naderi, G. B., Dunning, B. E., Mangold, B. L., Mone, M. D., Russell, M. E., Weldon, S. C. & Hughes, T. E. (2002). *J. Med. Chem.* **45**, 2362–2365.